IEEE 802.11n: Performance Analysis with Spatial Expansion, Receive Diversity and STBC

Roger Pierre Fabris Hoefel

Department of Electrical Engineering
Federal University of Rio Grande do Sul (UFRGS)
roger.hoefel@ufrgs.br

***Abstract*— In this paper, we investigate the effects of transmit antenna correlation, receive antenna correlation, frequency selectivity and imperfect synchronization and channel estimation schemes on the performance of IEEE 802.11n systems with spatial expansion, receive diversity and space-time block codes. The simulations results are validated using a first order analytical modeling.**

Keywords—802.11n; OFDM; MIMO; STBC; TGn channels

I. INTRODUCTION

The IEEE 802.11 amendment [1] allows a maximum gross physical layer (PHY) data rate of 260 Mbps [2, p. 100] and 540 Mbps [2, p. 140] within 20 MHz and 40 MHz bandwidth, respectively, when orthogonal frequency division multiplexing (OFDM) multiple input multiple output (MIMO) spatial division multiplexing (SDM) transmission scheme with four layers is implemented [3]. These high data rates demand a signal-to-noise ratio (SNR) greater than 40 dB at the input of Viterbi convolutional decoder for a typical packet error rate (PER) of 1% when a SDM MIMO 4x4 scheme with linear minimum mean squared error (MMSE) equalization and binary convolutional code (BCC) is assumed [4]. However, in the extremely competitive global broadband wireless market with low profit margins, it is not cost effective to design hardware to provide an SNR above 35 dB due to noise figure (NF) and other implementation impairments in the analog radio-frequency (RF) frontend and analog-to-digital converters (ADC) [2, p. 120].

The aim of this paper is to analyze the performance of IEEE 802.11n optional techniques of receive diversity (RxD), space-time block coding (STBC) and spatial expansion (SE) in order to reduce the target SNR at high throughput (HT) 802.11n receiver input, and, therefore, improving the system reliability and coverage. To accomplish our objectives this paper is organized as follows. Section II summarizes previous works in this field in order to contextualize the main contributions and relevance of this paper. Section III points out fundamental aspects of the IEEE 802.11n PHY layer for reader's convenience. Section IV describes the transceivers schemes analyzed in this paper. In Section V, firstly an IEEE 802.11n PHY simulator is validated. In the following, an extensive performance analyzes of the IEEE 802.11n system with RxD, STBC and SE techniques is carried out. Finally, our conclusions are drawn in Section VI.

II. PREVIOUS WORKS, MAIN CONTRIBUTION AND RELEVANCE

We have an absolute consciousness that STBC schemes have been researched for a long time and clearly described in many excellent papers and research books [5]. However, there are few papers on the singularities and tradeoffs related to the application of STBC in the IEEE 802.11n amendment.

The implementation of STBC schemes using the 802.11n PHY layer proposed by the WWiSE (World Wide Spectral Efficiency) was investigated in [6]. In this paper was analyzed a MIMO 4x4 using ½ STBC code rate and MIMO 2x2 using STBC with code rate 1 under flat and frequency selective Rayleigh fading channels. A channel with time diversity was assumed, what it is no applicable to indoor environments. The authors concluded that a MIMO 4x4 scheme with ½ STBC code rate allows a power gain in comparison with MIMO 2x2 with 1 STBC code rate due to the time diversity.

The effects of TGn channel models on STBC 2x1 and STBC 2x2 bit error rate (BER) were investigated in [7]. The authors did not simulate the 802.11n amendment, but only focused on the STBC performance for uncoded quaternary phase-shift keying (QPSK) signaling and the throughput for QPSK with binary convolutional code (BCC) with code rate ¾.

We believe that the most complete performance analysis in the open literature that follows strictly the IEEE 802.11n amendment was carried out by *Perahia* and *Stacey* in their excellent research book [2], where extensive results on STBC performance over the TGn channel model B were presented and analyzed [2, p. 147]. Hence, the main contributions of our paper are: *(1)* to validate the results shown in [2] using analytical and simulation tools; *(2)* to analyze the performance of 802.11n with RxD, STBC and SE for other TGn channel models to verify the effects of transmit and receive antenna correlation and different levels of frequency selectivity on the performance of IEEE 802.11n system assuming realistic synchronization and channel estimation schemes.

III. IEEE 802.11N PHY LAYER

A. SNR FOR OFDM MIMO 802.11N SYSTEM

The SNR for the 802.11n system can be expressed as [4]

$$SNR = \frac{E_b}{N_0}\left(\frac{N_{data}+N_{pilot}}{N_{FFT}}\right)(N_{BPSCS}\, r), \quad (1)$$

where E_b is the energy per bit and N_0 is the variance of the zero-mean circular symmetric complex Gaussian (ZMCSCG) random variable (r.v). For a bandwidth of 20 MHz, the remaining parameters are: Fast Fourier Transform length (N_{FFT}) of 64 samples; number of data subcarrier (N_{data}) equals to 52; number of pilot subcarriers (N_{pilot}) equals to 4; N_{BPSCS} is the number of bits per subcarrier per stream (i.e., the modulation cardinality); r denotes the code rate of the BCC.

B. IEEE 802.11SIMULATOR

We have been developing a simulator in Matlab and ANSI C that follows the IEEE 802.11n amendment in its fundamental structure [1-2], only eliminating signal processing operations that are not essential for a baseband discrete time simulation.

978-1-4673-1881-5/12/$31.00 ©2012 IEEE

The mandatory blocks of the 802.11n transmitter are shown in Fig. 1. The simulator implements the *scrambler* [1, p. 65]; *the* BCC with bit puncturing [1, p. 288]; *the stream parser* is responsible for the separation of the coded bits into spatial streams [1, p. 293]; *the interleaver* is applied to the coded bits for each OFDM symbol at the output of the stream parser [1, p. 294]; *the constellation mapper* maps coded bits into constellation points, resulting in complex data symbols transported in each OFDM subcarrier [1, p. 295]; *the optional STBC block after the Mapper* (not shown in Fig. 1) implements the spatial-time coding where the spatial streams (SS) are mapped to space-time streams (STS) [1, p. 296]; *the optional spatial mapping* after STBC (not shown in Fig. 1) implements the SE [1, p. 298], as detailed in next section; *four pilots* are inserted to tracking the residual phase due to imperfect synchronization [1, p. 297], [4]; *the inverse Fast Fourier Transform (IFFT)* converts each OFDM symbol to the time domain [1, p. 301]; *the cyclic shift diversity (CSD)* is necessary to decorrelate the signals transmitted at each STS to mitigate the undesirable beamforming effects [1, p. 283]; *the cyclic prefix (CP)* is added using the final samples of each OFDM symbol [1, p. 262]. The preamble is put in front of the data field, creating a complete HT mixed format packet [1, p. 271], which is backward compatible with IEEE 802.11a/g amendments.

The receiver structure is not defined in the IEEE 802.11n amendment. Fig. 2 depicts the receiver architecture used in this paper. The joint time-frequency synchronization scheme and the channel estimation scheme are described in [4]. The metrics for soft-decision Viterbi decoding are calculated using the methodology proposed in [8].

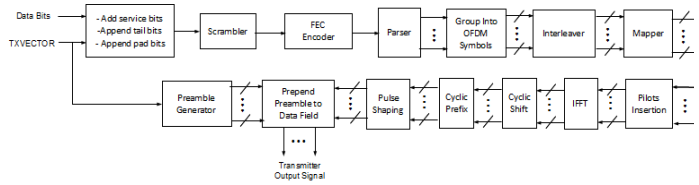

Figure 1. Block diagram of an IEEE 802.11n transmitter [1, p. 261].

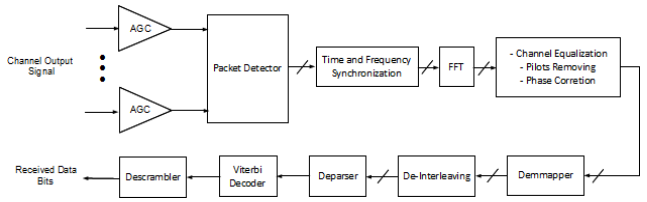

Figure 2. Block diagram of an IEEE 802.11n receiver.

IV. STBC, Receive Diversity And Spatial Expansion

A. STBC Schemes

The 802.11n amendment defines spatial stream (SS) as "One of several streams of bits or modulation symbols that may be transmitted over multiple spatial dimensions that are created by the use of multiple antennas at both ends of a communications link" [1, p. 3]. The number of SS is denoted by N_{SS}. The number of the streams at the output of the STBC N_{TS} is labeled as space-time streams, defined in the 802.11n amendment as "Streams of modulation symbols created by applying a combination of spatial and temporal processing to one or more spatial streams of modulation symbols" [1, p. 3].

Tab. I summarizes the STBC schemes investigated in this paper: *(1)* SBTC 2x1 – N_{ss}=1 and N_{TS}=2; (*2)* SBTC 3x2 - N_{ss}=2 and N_{TS}=3; (*3)* SBTC 4x2 - N_{ss}=2 and N_{TS}=4; (*4)* SBTC 4x3 - N_{ss}=3 and N_{TS}=4. The STBC 2x2 configuration, that has N_{ss}=1 and N_{TS}=2 and one additional receive antenna for spatial diversity, is also analyzed. The superscript * in Tab. I denotes complex conjugate.

TABLE I
STBC CONFIGURATION: TRANSMITTED SYMBOL FOR EACH SYMBOL TIME AT EACH TRANSMIT ANTENNA

	Symbol Time t_1				*Symbol Time t_2*			
Tx Antenna	*1*	*2*	*3*	*4*	*1*	*2*	*3*	*4*
STBC 2x1	x_1	$-x_2^*$	---	---	x_2	x_1^*	---	---
STBC 3x2	x_1	$-x_2^*$	x_3	---	x_2	x_1^*	x_4	---
STBC 4x2	x_1	$-x_2^*$	x_3	$-x_4^*$	x_2	x_1^*	x_4	x_3^*
STBC 4x3	x_1	$-x_2^*$	x_3	x_5	x_2	x_1^*	x_4	x_6

The received signal for the STBC system can be described using a vector notation. The signal processing must be carried per OFDM subcarrier. However, in this paper we drop the notation that specifies the *k*th subcarrier to avoid a cumbersome notation. As an illustrative example, for the STBC 3x2 system the equalizer must deal with the following vector [2, p.154]:

$$\begin{bmatrix} y_1 \\ y_2^* \\ y_3 \\ y_4^* \end{bmatrix} = \sqrt{\frac{SNR}{3}} \cdot \begin{bmatrix} h_{11} & -h_{12} & h_{13} & 0 \\ h_{12}^* & h_{11}^* & 0 & h_{13}^* \\ h_{21} & -h_{22} & h_{23} & 0 \\ h_{22}^* & h_{21}^* & 0 & h_{23}^* \end{bmatrix} \cdot \begin{bmatrix} x_1 \\ x_2^* \\ x_3 \\ x_4^* \end{bmatrix} + \begin{bmatrix} z_1 \\ z_2^* \\ z_3 \\ z_4^* \end{bmatrix}, \quad (2)$$

where y_1 and y_2 are the symbols at receive antenna 1in the symbol times t_1 and t_2, respectively; y_3 and y_4 are the symbols at receive antenna 2 in the symbol times t_1 and t_2, respectively. The complex channel gain between the *j*th transmit antenna and the *i*th receive antenna is denoted by h_{ij}. The column noise vector $z = [z_1, , \cdots, z_4]^T$is a ZMCSCG with variance N_0. The vector/ matrix modeling for the other STBC configurations can be found in [2, p. 154].

In this paper, the STBC equalizer uses the weight matrix based on the zero-forcing (ZF) [9, p. 349]:

$$\boldsymbol{W_{ZF}} = \left(\tilde{\boldsymbol{H}}^{\boldsymbol{H}}\tilde{\boldsymbol{H}}\right)^{-1}\tilde{\boldsymbol{H}}^{\boldsymbol{H}}, \quad (3)$$

where $(.)^H$ denotes the Hermitian transpose operation. The estimated channel matrix is denoted by $\tilde{\boldsymbol{H}}$. It is used ZF instead of MMSE because we have concluded that is more feasible to implement ZF equalization with minor performance degradation for architectures that mix transmit diversity with SDM (e.g., STBC 4x2).

B. Space Division Multiplexing with Receive Diversity

The SDM MIMO systems investigated in this paper implement a MMSE receiver since it presents a highly superior performance in relation to ZF for SDM MIMO without STBC [4]. Therefore, the receive MMSE weight matrix is given by

$$\boldsymbol{W_{MMSE}} = \left[\tilde{\boldsymbol{H}}^{\boldsymbol{H}}\tilde{\boldsymbol{H}} \quad + \frac{\boldsymbol{I_{N_{rx}}}}{\boldsymbol{SNR}}\right]\tilde{\boldsymbol{H}}^{\boldsymbol{H}}, \quad (4)$$

where $\boldsymbol{I_{N_{rx}}}$ is the square identity matrix of order N_{rx} , where N_{rx} is the number of receive antennas [9, p.356].

In this paper, the performance of MIMO SDM is analyzed using the following configurations: *(1)* single input single output system (SISO) with 1 SS and 1 STS; *(2)* single input multiple output system (MISO) with 1 SS and 1 STS; *(3)* MIMO 2x2 with 2 SS and 2 STS; *(4)* MIMO 2x3 with 2 SS, 2 STS and one additional receive antenna for spatial diversity; (*5*) MIMO 2x4 with 2 SS, 2 STS and two additional receive antennas for spatial diversity; (*6*) MIMO 3x4 with 3 SS, 3 STS and one additional antenna for spatial diversity.

C. Spatial Expansion

The IEEE 802.11n specifies a sounding technique to estimate the channel between the transmitting station (STA) and receiving STA [1, p. 161]. The sounding algorithm can signalize that the MIMO channel matrix is not well-conditioned [9, p. 295] and, therefore, using SDM MIMO in the sounded channel realization is not suitable. One possible solution is to use the optional STBC scheme, as described in the earlier subsection. The simplest solution would be not use all transmit antennas. However, this naive approach would lose power since HT 802.11n devices implement one RF amplifier per antenna chain. To avoid this power loss, the IEEE 802.11 amendment implements the optional SE technique, where "vectors of constellation points from all the space-time streams are expanded via matrix multiplication to produce the input to all the transmit chains" [1, p. 261]. The spatial mapping necessary to implement the SE scheme is fully described in [1, p. 298]. For instance, the matrix D used to map 2 SS (N_{SS}=2) to 3 transmit antennas (N_{TX}=N_{TS}= 3) is given by

$$D = \sqrt{\frac{2}{3}} \cdot \begin{bmatrix} 1 & 0 \\ 0 & 1 \\ 1 & 0 \end{bmatrix}, \quad (5)$$

where the multiplicative constant is used to normalize the power.

V. Performance Analyses

A. *Validation of the IEEE 802.11n Simulator*

The analytical results shown in this paper were obtained using equations (16) to (20) of [4]. In this paper, a medium access control (MAC) packet data unit (MPDU) payload of 1024 bytes is assumed.

Fig. 3 shows analytical (white symbols) and simulation (black symbols) results for MPDU PER as a function of the SNR in dB with single input single output (SISO) matched filter (MF), maximum ratio combiner (MRC) 1x2 and STBC 2x1 transceivers over canonical quasi-static flat fading Rayleigh channels. It is assumed the modulation code scheme 0 (MCS0: N_{SS}=1, BPSK using BCC with code r=1/2) and MCS7 (N_{ss}=1, 64-QAM, BCC with r=5/6) with ideal synchronization and perfect channel estimation. These results allow inferring the following conclusions: *(1)* a perfect (approximated) agreement between analytical and simulation results for MCS0 (MCS7) with both MF and MRC receivers; *(2)* the SBTC scheme has a power loss of 3 dB in relation to the MRC receiver, as expected theoretically; *(3)* the STBC scheme allows a power gain of 8 dB and 10 dB for MCS0 and MCS7, respectively, in relation to the SISO MF receiver;*(4)* the MCS7 demands a SNR increase of approximately 20 dB and 19 dB in relation to the MCS0 when it is implemented the SISO MF and MRC receivers, respectively.

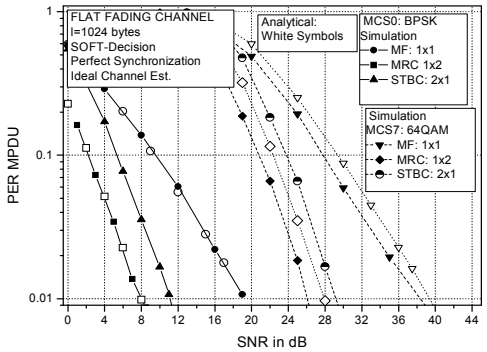

Figure 3. Analytical and simulation results for the MPDU PER as a function of SNR in dB for the quasi-static flat fading Rayleigh channel model.

B. Results for the MPDU PER: Receive Diversity and STBC

TGn B channel models residential environments with maximum delay τ_{max} of 80 ns and root mean square (rms) delay spread τ_{rms} of 15 ns [2, p. 36, p. 53]. This channel has an envelope correlation of ρ_{tx}= 0.9 for the transmitter side and ρ_{rx}= 0.88 for the receiver side when it is assumed uniform linear antenna (ULA) arrays with antenna separation of half-wavelength (λ/2) [7].

Fig. 4 shows results for the TGn B channel in order to compare the performance of SISO MF, SISO MMSE, MRC 1x2, MMSE 1x2 and STBC 1x2 transceivers. It is assumed MCS0 and MCS7 with realistic synchronization and channel estimation schemes [4]. Theoretically, the MF and MRC receivers have the optimal performance over ideal conditions (i.e., perfect synchronization and channel estimation). However, it can be seen that the MMSE receiver has a superior performance in relation to MF and MRC receivers for both SISO and SIMO environments since it can better cope with the inter-carrier interference caused by the non-ideal synchronization and imperfect channel estimation. As expected analytically, the STBC 2x1 scheme has a power loss of approximately 3 dB in relation to the MMSE 2x1 scheme. Finally, we concluded that the spatial diversity provided by the MMSE 1x2 and STBC 1x2 transceivers allows a huge performance improvement in relation to the SISO MMSE scheme for both MCS0 and MCS7.

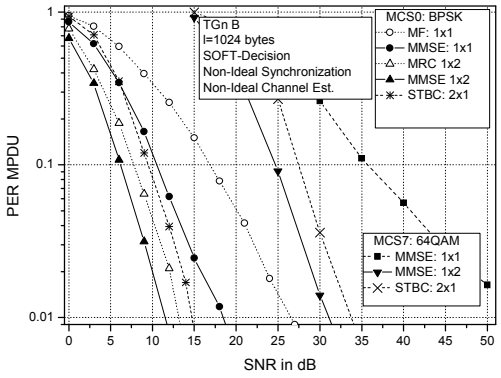

Figure 4. Simulation results for the MPDU PER as a function of SNR in dB under the TGn B channel model: MF and MMSE SISO receivers; MRC and MMSE SIMO 1x2 receivers and STBC 2x1 scheme.

TGn C channel models small offices with τ_{max}=*200 ns* and τ_{rms}=*30 ns* [2, p. 53]. This channel has low envelope correlation for the transmitter side (ρ_{tx}= *0.47*) and larger envelope correlation for the receiver side (ρ_{rx}= *0.73*) for λ/2 ULA arrays [7].

TGn E channel models multi-story offices with τ_{max}=*730 ns* and τ_{rms}=*100 ns* [2, p. 55]. This channel presents correlated envelope for the transmitter side (ρ_{tx}= *0.88*) and uncorrelated envelope at the receiver side (ρ_{rx}= *0.35*) for λ/2 ULA arrays [7].

Fig. 5a shows simulation results for the channel models TGn C and E in order to compare the performance of MMSE SISO, MMSE SIMO 1x2 and STBC 2x1 transceiver architectures. It is assumed MCS0 with realistic synchronization and channel estimation schemes. These results allow inferring interesting conclusions: *(1)* the frequency diversity explains the superior performance attainable under TGn E in the SISO environment; *(2)* the STBC 2x1 scheme presents a performance degradation of 6 dB and 7 dB for a PER of 1% in relation to the MMSE 1x2 scheme over TGn C (ρ_{tx}=*0.47*) and E (ρ_{tx}=*0.88*) channels, respectively; *(3)* the MMSE 1x2 receiver allows an expressive power gain of 6 dB for a PER of 1% over the TGn C channel, while the STBC 2x1 scheme allows a power gain of only 0.5 dB

in relation to SISO MMSE receiver; *(4)* the MMSE 1x2 scheme has a power gain of 5 dB in relation to the SISO receiver over TGn E channel, while the STBC 1x2 degrades the performance in 1.5 dB. Note that this interesting characteristic occurs because into this range of the SNR it is not possible to decouple the transmitted spatial-temporal coded symbols due to the imperfect channel estimation in this highly frequency selective TGn E channel.

Fig. 5b is analogous to Fig. 5a, expect that now the MCS7 is assumed instead of MCS0. Results for the STBC 2x2 scheme are also included. First, we observe that using transmit and/or receive diversity provides a huge performance gain in relation to the SISO scenario. For the channel TGn C (uncorrelated transmit antennas and correlated receive antennas) the STBC 2x1 scheme demands 2 dB more power in relation to the MMSE 1x2 scheme. However, for the channel TGn E (correlated transmit antennas and uncorrelated receive antennas) the STBC 2x1 scheme demands 5 dB more power to have the same 1% PER obtained with the MMSE 1x2 receiver. We also have observed that practically the same performance is attainable with STBC 2x2 and MMSE 1x2 receivers over the TGn E channel (i.e., the STBC 2x2 has a power gain of 5.0 dB in relation to the STBC 2x1 scheme). Finally, we observed that the gain of the STBC 2x2 scheme in relation to STBC 2x1 is decreased to 4 dB under TGn C channel due to the higher envelope correlation at receiver side.

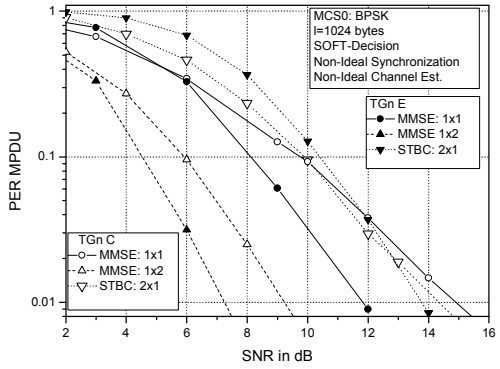

Figure 5a. MMSE SISO, MMSE SIMO 1x2 and STBC 2x1 transceivers with MCS0 (N_{SS}=1, BPSK, BCC with r=1/2).

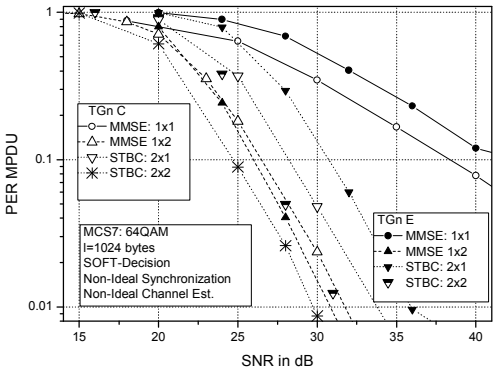

Figure 5b. MMSE SISO, MMSE SIMO 1x2; STBC 2x1 and STBC 2x2 transceivers with MCS7 (N_{SS}=1, 64-QAM, BCC with r=5/6).

Figure 5. Simulation results for the MPDU PER as a function of SNR under TGn C e TGn E channel models.

Tab. II shows the values of the SNR in dB necessary for a PER of 1% for MMSE 1x2 and STBC 2x1 schemes with MCS7. The STBC 2x1 presents a power loss of 2 dB in relation to the MMSE 1x2 over TGn C channel (ρ_{tx}= *0.47*) that is lower than the power loss of 5 dB observed over the TGn E channel (ρ_{tx}=*0.88*). The frequency diversity explains why the MMSE 1x2 scheme presents a superior performance over TGn E channel (τ_{rms}=*100 ns*) in relation to that one observed for the flat fading spatially correlated TGn A channel.

TABLE II
SNR NECESSARY FOR A PER OF 1% WITH MCS7.

Receiver	*TGn A*	*TGn B*	*TGn C*	*TGn E*
MMSE: 1x2	33.0	31.0 dB	32.0 dB	31.0 dB
STBC: 2x1	37.0	34.0 dB	34.0 dB	36.0 dB

Fig. 6 shows the MPDU PER versus the SNR in dB for the MMSE 2x2, MMSE 2x3 and STBC 3x2 transceivers over TGn B and C channels. It is assumed MCS 15 (N_{SS}=2, 64-QAM, BCC with r=5/6). Firstly, we have observed that for both channels the performance of MMSE 2x2 scheme is not satisfactory even with an unfeasible SNR of 50 dB. Second, we have verified for both channels that the MMSE 2x3 transceiver allows an expressive power gain in relation to the SISO case due to the receive diversity. However, note that for a PER of 1% the TGn C channel demands 3.5 dB more in relation to channel TGn B due to the deleterious effects of greater frequency selectivity on the accuracy of the least square (LS) channel estimation scheme [2, p. 94]. Finally, comparing the performance of MMSE 2x3 and STBC 3x2 schemes, we have verified that the later scheme has a power loss of 7.0 dB and 6.5 dB for TGn B and C channels, respectively. This power loss greater than 3 dB occurs due to the joint effects of antenna correlation and imperfect channel estimation due to the frequency selectivity and low matrix conditioning.

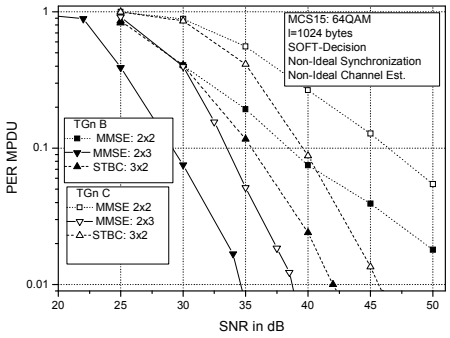

Figure 6. Simulation results for the MPDU PER as a function of SNR under TGn B and TGn C channel models: MMSE 2x2, MMSE MIMO 2x3; STBC 3x2 transceivers with MCS 15 (N_{SS}=2, 64-QAM, BCC with r=5/6).

Fig. 7 shows the MPDU PER versus the SNR in dB for the MMSE 2x2, MMSE 2x4 and STBC 4x2 transceivers over TGn B and C channels. Comparing these results with the ones shown in Fig. 6 for a reference PER of 1%, we have concluded that transmit (TxD) and receive (RxD) diversity causes the following effects on the PER: (*1*) for the TGN B channel there is a power gain of 5 dB and 3 dB with the implementation of MMSE 2x4 (increase of RxD) and STBC 4x2 (increase of TxD) transceivers, respectively, instead of MMSE 2x3 and STBC 3x2 transceivers; (*2*) the gains attainable over a TGn C channel for both receivers are lower (e.g., 3 dB for MMSE 2x4 and 2.5 dB for STBC 2x3) due to the effects of the greater frequency selectivity of this channel in relation to TGn B channel. Note that both channels have high envelope correlation at receive side.

Fig. 8 shows the MPDU PER versus the SNR in dB for the MMSE 3x3, MMSE 3x4 and STBC 4x3 transceivers over TGn B and C channels. MCS23 (N_{SS}=3, 64QAM, BCC with r=5/6) is assumed. Comparing these results with the ones shown in Fig 7,

we can verify that the use of one more spatial stream demands an expressive increase in the SNR (e.g., assuming a PER of 1% and channel TGn B, then the MMSE 3x4 and STBC 3x4 schemes demand an increase in SNR of 11 dB and 7.5 dB, respectively, in relation to that one necessary for MMSE 2x4 and STBC 4x2 schemes). Finally, a power loss of 3 dB between STBC 4x3 and MMSE 3x4 schemes over the TGn B channel is observed.

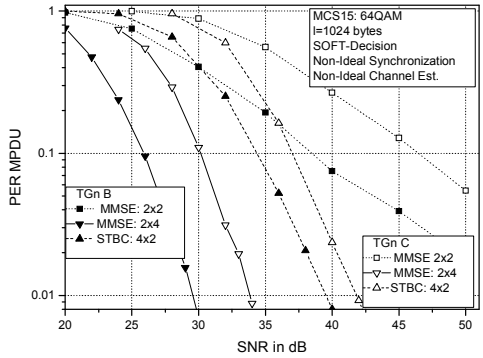

Figure 7. Simulation results for the MPDU PER as a function of SNR under TGn B e TGn C channel models: MMSE MIMO 2x2, MMSE MIMO 4x2; STBC 4x2 transceivers with MCS 15 (N_{SS}=2, 64-QAM, BCC with r=5/6).

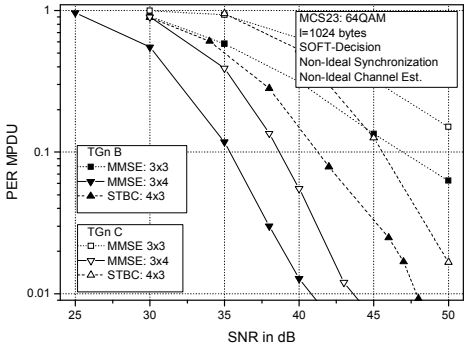

Figure 8. Simulation results for the MPDU PER as a function of SNR under TGn B and TGn C channel models: MMSE MIMO 3x3, MMSE MIMO 3x4; STBC 4x3 transceivers with MCS 23 (N_{SS}=3, 64-QAM, BCC with r=5/6)

Tab. III compares the simulation results presented in this paper with the ones showed in [2]. The close agreement has a fundamental importance since it corroborates the correctness of both simulation results obtained using independent implementations of a complex IEEE 802.11n PHY layer simulator. We emphasize that *E. Perahia* and *R. Stacey* presented only results for the TGn B channel model, while we have extended their results for flat fading, TGn C and E channel models, besides validating the IEEE 802.11n simulator analytically (cf. Fig. 3).

TABLE III
SNR NECESSARY FOR A PER OF 1% OVER A TGN B CHANNEL.

Receiver	*Sml.*	*Ref. [2]*	*Receiver*	*Sml.*	*Ref. [2]*
MMSE: 1x2 (MCS 7)	31.5 dB	31.0 dB	*MMSE: 4x2 (MCS 15)*	29.5 dB	32.0 dB
STBC: 2x1 (MCS 7)	34.0 dB	34.0 dB	*STBC: 4x2 (MCS 15)*	39.0 dB	37.0 dB
MMSE: 2x3 (MCS 15)	34.5 dB	35.5 dB	*MMSE: 3x4 (MCS 23)*	41.0 dB	40.0 dB
STBC: 2x3 (MCS 15)	42.0 dB	39.5 dB	*STBC: 3x4 (MCS 23)*	47.5 dB	47.0 dB

C. Results for the MPDU PER: Spatial Expansion (SE)

Fig. 9 compares the performance between MIMO 2x2 (i.e., N_{SS}=2, N_{TX}=N_{Rx}=2) and SE 3x2 (i.e., N_{SS}=2, N_{TX}=3 and N_{Rx}=2) schemes for MCS8 (N_{SS}=2, BPSK, BCC with r=1/2) and MCS13 (N_{SS}=2, 16-QAM, BCC with r=1/2) over canonical Rayleigh flat fading and TGn B channels. The SE 3x2 transmission scheme allows a power gain of 2.5 dB (5 dB) with MCS8 (MCS13) for a PER of 1% under the flat fading Rayleigh channel because the same information transmitted in two antennas with CS produces an observable frequency diversity at receiver input. For the TGn B channel there is no expressive power gain since the channel already has some degree of frequency diversity in the MIMO 2x2 environment. However, the SE technique allows that all transmitter RF chains be used, which permits that all available power at the transmitter side be effectively used. Results do not show in this paper due to space constraints indicate that the SE 2x1 allows a power gain of 3 dB in relation to MIMO 1x1 over TGn B channel since the SISO TGn B channel presents a minor frequency diversity.

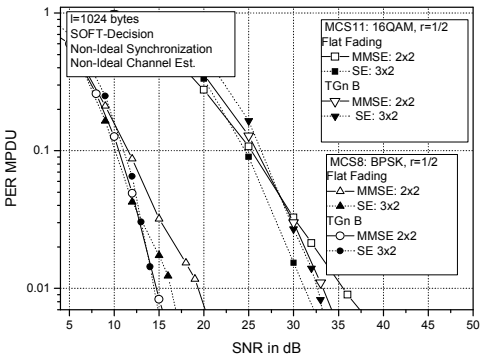

Figure 9. Simulation results for the MPDU PER as a function of SNR under flat fading, and TGn B channel models: MMSE 2x2 and SE 3x2.

VI. CONCLUSIONS

In this paper, we analyzed the performance of spatial expansion, receive diversity and STBC transceiver architectures designed to reduce to the SNR at HT IEEE 802.11.n receiver input into a feasible range. Simulation results, validated by analytical modeling, show that it is fundamental to implement a robust sounding scheme to dynamically set up the transceiver configuration since the relative performance of the transceiver architectures depend strongly on the stochastic characteristic of the observable channel realization, such as, transmit and receive antenna correlation and delay spread of the multipath channel.

REFERENCES

[1] Wireless LAN Medium Access Control (MAC) and Physical Layer (PHY) Specifications, Amendment 5: Enhancement for Higher Throughput, IEEE Std 802.11n-2009, 2009.

[2] E. Perahia, R. Stacey, *Next Generation Wireless LANS*, New York, USA, Cambridge University Press, 2008.

[3] A. Gravalos et al. "Spatial data stream multiplexing scheme for high-throughput WLANs," *IET Communications,* v.2, no.9, pp. 1177-1185, 2008.

[4] R. P. F. Hoefel. "On the synchronization of IEEE 802.11n devices over frequency selective TGn channel models," *25th Annual Canadian Conference on Electrical and Computer Engineering (CCECE 2012),* Montreal, 2012

[5] E. G. Larsson and P. Stoica. *Space-Time Block Coding for Wireless Communication,* Cambrdge, UK: Cambridge University Press, 2003.

[6] A. G. Gravalos, M. G. Hadjinicolaou and Q. Ni, "Performance analyses of IEEE 802.11n under different STBC rates using 64-QAM*," 2nd International Symposium on Wireless Pervasive Computing*, ISWPC-07, 2007.

[7] I. Vermesan, A. Moldovan, T. Palade and R. Colda, "Multi antenna STBC transmission technique evaluation under IEEE 802.11n conditions," *2010 15th International Conference on Microwave Techniques (COMITE),* 2010.

[8] F. Tosato and P. Bisagli, "Simplified soft-output demapper for binary interleaved COFDM with applications to HIPERLAN/2," *IEEE International Conference on Communications 2002*, 2002.

[9] D. Tse and P. Viswanath, *Fundamentals of Wireless Communication,* New York, USA: Cambridge Press, 2005.